

Indirect study of ^{19}Ne states near the $^{18}\text{F}+p$ threshold.

N. de Séréville^{a,1} A. Coc^a C. Angulo^b M. Assunção^a D. Beaumel^c
 E. Berthoumieux^d B. Bouzid^e S. Cherubini^{b,2} M. Couder^{b,3} P. Demaret^b
 F. de Oliveira Santos^f P. Figuera^g S. Fortier^c M. Gaelens^{b,4}
 F. Hammache^{h,5} J. Kiener^a A. Lefebvre-Schuhl^a D. Labarⁱ P. Leleux^b
 M. Loiselet^b A. Ninane^b S. Ouichaoui^e G. Ryckewaert^b N. Smirnova^j
 V. Tatischeff^a

^aCSNSM, IN2P3/CNRS and Université Paris Sud, F-91405 Orsay campus, France

^bCentre de Recherches du Cyclotron and Institut de Physique Nucléaire, Université catholique de
 Louvain, B-1348 Louvain-la-Neuve, Belgium

^cIPN, IN2P3/CNRS, and Université Paris Sud, F-91406 Orsay Cedex, France

^dCEA, DAPNIA/SPhN, F-91191 Gif/Yvette Cedex, France

^eUSTHB, B.P. 32, El-Alia, Bab Ezzouar, Algiers, Algeria

^fGANIL B.P. 5027, 14021 Caen Cedex, France

^gLaboratori Nazionali del Sud, INFN, Via S. Sofia, 44 - 95123 Catania, Italy

^hGSI mbH, Planckstr. 1, D-64291 Darmstadt, Germany

ⁱUnité d'Imagerie Moléculaire et Radiothérapie Expérimentale, Université catholique de Louvain,
 B-1348 Louvain-la-Neuve, Belgium

^jDepartment of Subatomic and Radiation Physics, University of Ghent, Proeftuinstraat 86, B-9000
 Ghent, Belgium

Abstract

The early $E \leq 511$ keV gamma-ray emission from novae depends critically on the $^{18}\text{F}(p,\alpha)^{15}\text{O}$ reaction. Unfortunately the reaction rate of the $^{18}\text{F}(p,\alpha)^{15}\text{O}$ reaction is still largely uncertain due to the unknown strengths of low-lying proton resonances near the $^{18}\text{F}+p$ threshold which play an important role in the nova temperature regime. We report here our last results concerning the study of the $d(^{18}\text{F},p)^{19}\text{F}(\alpha)^{15}\text{N}$ transfer reaction. We show in particular that these two low-lying resonances cannot be neglected. These results are then used to perform a careful study of the remaining uncertainties associated to the $^{18}\text{F}(p,\alpha)^{15}\text{O}$ and $^{18}\text{F}(p,\gamma)^{19}\text{Ne}$ reaction rates.

Key words: Transfer reaction, Radioactive beam, DWBA, Spectroscopic factor, Nova nucleosynthesis.
PACS: 26.60.Je, 21.10.Jx, 26.30.+k, 27.20+n

1. Introduction

Gamma-ray emission from classical novae is dominated, during the first hours, by positron annihilation resulting from the beta decay of radioactive nuclei. The main contribution comes from the decay of ^{18}F (half-life of 110 min) and hence is directly related to ^{18}F formation during the outburst [1, 2, 3]. A good knowledge of the nuclear reaction rates of production and destruction of ^{18}F is required to calculate the amount of ^{18}F synthesized in novae and the resulting gamma-ray emission. The relevant reactions for the ^{18}F production [$^{17}\text{O}(\text{p},\gamma)^{18}\text{F}$ and $^{17}\text{O}(\text{p},\alpha)^{14}\text{N}$] have been recently studied [4, 5, 6] and point to a lower production of ^{18}F . The relevant rates for the ^{18}F destruction are the $^{18}\text{F}(\text{p},\gamma)^{19}\text{Ne}$ reaction ($Q = 6.411$ MeV) and the much faster $^{18}\text{F}(\text{p},\alpha)^{15}\text{O}$ reaction ($Q = 2.822$ MeV). In order to calculate these destruction rates, it is important to determine the properties of the ^{19}Ne states near the $^{18}\text{F} + \text{p}$ threshold. Therefore, an extensive series of experiments like (p,p) elastic scattering [7, 8, 9], direct (p, α) measurements [8, 9, 10, 11, 12, 13] and indirect transfer reactions to populate levels in ^{19}Ne and ^{19}F [14, 15, 16, 17] have been performed. However, its rate remains poorly known at nova temperatures (lower than 3.5×10^8 K) due to the scarcity of spectroscopic information for levels near the proton threshold in the compound nucleus ^{19}Ne . This uncertainty is directly related to the unknown properties of the first three levels in ^{19}Ne : $E_x, J^\pi = 6.419$ MeV, ($3/2^+$); 6.437 MeV, ($1/2^-$) and 6.449 MeV, ($3/2^+$) (see Fig 1) and following Utku et al. [14] we will assume the previous spin and parity assignments even though they have not been measured directly. The tails of the corresponding resonances at $E_r = 8, 26$ and 38 keV, respectively, can dominate the $^{18}\text{F}(\text{p},\alpha)^{15}\text{O}$ astrophysical S-factor in the relevant energy range [3]. As a consequence of these nuclear uncertainties, the ^{18}F production in nova and the early gamma-ray emission was estimated to be uncertain by a factor of ≈ 300 [3].

In order to estimate the level position and spectroscopic factors of the relevant states in ^{19}Ne , we performed shell-model calculations with the OXBASH code [18]. It was not possible to reproduce experimental levels at energies about 6–7 MeV, motivating hence an experimental approach. Due to the very low Coulomb barrier penetrability for the relevant resonances in ^{19}Ne , a direct measurement of their strength is at present impossible. Hence, we have used an indirect method, the $\text{d}(^{18}\text{F},\text{p})^{19}\text{F}$ transfer reaction, aiming at the determination of the one-nucleon spectroscopic factor (S) in the analog levels of the ^{19}F mirror nucleus. Assuming the equality of the spectroscopic factors in analog levels, it is possible to calculate the ^{19}Ne proton widths through the relation $\Gamma_p = S \times \Gamma_{\text{s.p.}}$ [19, 20] where $\Gamma_{\text{s.p.}}$ is the single particle width. Preliminary results were presented in [15], here we provide a detailed data analysis.

This paper is organized as follows. The experimental method is detailed in Sections 2 and 3. The data analysis is presented in Sections 4 and 5 and the remaining uncertainties

* Corresponding author.

Email address: deserevi@fyfu.ucl.ac.be (N. de Séréville).

¹ Present address: Université catholique de Louvain, Louvain-la-Neuve, Belgium.

² Present address: Ruhr-Universität-Bochum, Bochum, Germany.

³ Present address: Nuclear Physics Department, University of Notre Dame, Indiana, USA.

⁴ Present address: International Brachytherapy, Seneffe, Belgium.

⁵ Permanent address: IPN, Orsay, France.

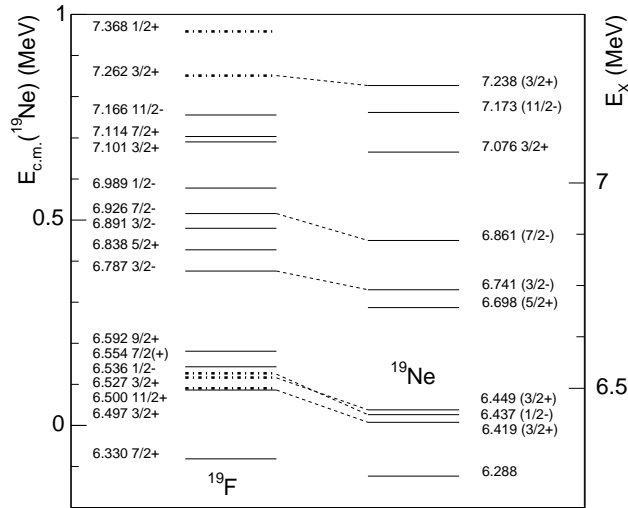


Fig. 1. Level scheme for ^{19}F and ^{19}Ne above the $^{18}\text{F} + \text{p}$ threshold. Dotted lines connect analog states from [14]. Dashed-dotted lines in ^{19}F represent the levels studied in the present work.

concerning the $^{18}\text{F}(\text{p},\alpha)^{15}\text{O}$ and $^{18}\text{F}(\text{p},\gamma)^{19}\text{Ne}$ reaction rates are studied in the concluding Section 6.

2. Experimental method

2.1. Experimental set-up

The experiment was performed at the CYCLONE RIB facility at the *Centre de Recherches du Cyclotron*, UCL, Louvain-la-Neuve, Belgium. We used a 14-MeV ^{18}F radioactive beam which was produced via the $^{18}\text{O}(\text{p},\text{n})^{18}\text{F}$ reaction, chemically extracted to form CH_3^{18}F molecules, transferred to an ECR source, ionized to the 2^+ state and then accelerated to the relevant energy [21]. The production of ^{18}F was made in the batch mode and an average of 2.2×10^6 ^{18}F ions per second on target was delivered for a total of 40 hours representing 15 ^{18}F batches. The beam contamination from its stable isobar ^{18}O was evaluated 20 hours after the delivery of the last batch from the counting rate on the target. The observed counting rate was in fact compatible with the ^{18}F radioactive decay and indicated a $^{18}\text{O} / ^{18}\text{F}$ ratio less than 10^{-3} .

The ^{18}F beam bombarded $100 \mu\text{g}/\text{cm}^2$ deuterated polyethylene (CD_2) targets. These targets were produced by polymerization and their thickness and homogeneity were checked by measuring the energy loss of α particles. The target stoichiometry and contamination were studied at the Orsay ARAMIS accelerator [22] after the $\text{d}(^{18}\text{F},\text{p})^{19}\text{F}$ experiment. Elastically scattered protons were detected with a silicon detector at a laboratory angle of 150° for an incident proton energy of 2.8 MeV [23, 24]. It was found that

the stoichiometry was not modified during the experiment as expected from the low ^{18}F beam intensity.

The products of the $d(^{18}\text{F},p)^{19}\text{F}$ reaction were detected using the multi-strip silicon detector LEDA [25]. Two configurations named LEDA and LAMP were used. These detectors are composed of 8 and 6 sectors, respectively, each divided into 16 radial strips. The energy calibration of the 224 strips was performed with a calibrated 3α -source (^{239}Pu , ^{241}Am and ^{244}Cm) whereas the time-of-flight calibration was performed with a precision pulser.

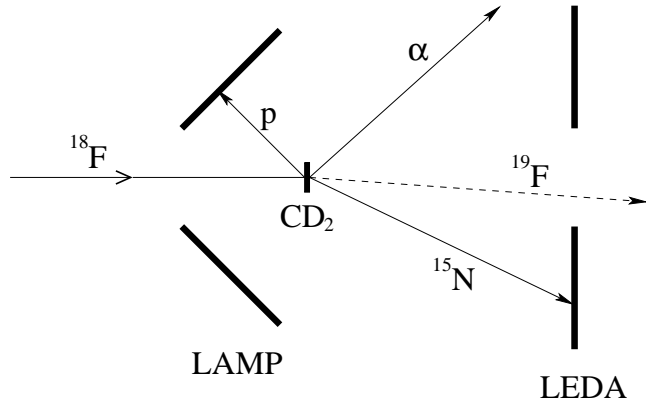


Fig. 2. The experimental set-up is shown with ^{18}F ions impinging on a CD_2 target. Protons were detected in LAMP while ^{15}N or α -particles from ^{19}F decay were detected in coincidence in LEDA. See Fig 1 in [15] for a perspective view of the set-up.

The experimental set-up is shown in Fig 2. The protons from the $d(^{18}\text{F},p)^{19}\text{F}$ reaction were detected in LAMP positioned 8.7-cm upstream from the target. It corresponds to laboratory angles between 110° and 157° , i.e. center-of-mass angles between 12° and 44° for the two $3/2^+$ levels of astrophysical interest. Since these two levels in ^{19}F are situated above the α -threshold at 4.013 MeV, they decay through $^{19}\text{F}^* \rightarrow \alpha + ^{15}\text{N}$. The decay products were detected in LEDA positioned 40-cm downstream from the target, which corresponds to laboratory angles between 7° and 18° . The positions of the detectors were determined by Monte-Carlo simulations: for LAMP, the angular range and detection efficiency were maximized and for LEDA, the coincidence efficiency between protons detected in LAMP and ^{15}N detected in LEDA was optimized.

Rutherford elastic scattering of ^{18}F on the carbon contained in the target, detected in LEDA, provides the (target thickness) \times (beam intensity) normalization. We used the strip at 15.7° in LEDA for which the solid angle is maximum and less sensitive to the exact position of the beam on the target. Furthermore, for this strip the elastic scattering peaks of ^{18}F and ^{12}C are well separated. The uncertainty on the normalization is mainly due to the position of the beam (± 2 mm) and is estimated to be of 7%.

Data were collected in event-by-event mode where the multiplicity, the angle, the deposited energy and the time of flight relative to the cyclotron radio-frequency were recorded, allowing an off-line analysis of single and coincidence events.

2.2. Data reduction

Thanks to the low ^{18}F energy ($E_{c.m.} = 1.4$ MeV), below the Coulomb barrier of the $^{18}\text{F} + ^{12}\text{C}$ and $^{18}\text{F} + \text{d}$ systems, only a few channels are opened: $\text{d}(^{18}\text{F},\alpha)^{16}\text{O}$, $\text{d}(^{18}\text{F},\text{p})^{19}\text{F}$, $\text{d}(^{18}\text{F},\text{p}\alpha)^{15}\text{N}$, $\text{d}(^{18}\text{F},\text{n})^{19}\text{Ne}$, and $\text{d}(^{18}\text{F},\text{n}\alpha)^{15}\text{O}$. Single and coincidence events have been analyzed but the coincidence condition between LAMP and LEDA (see Figure 3) allows to distinguish easily the events from these reactions. The two-body properties of the $\text{d}(^{18}\text{F},\alpha)^{16}\text{O}$ reaction can be observed as a linear correlation between the detected energies in LAMP and LEDA, which is not the case for the three-body $\text{d}(^{18}\text{F},\text{p}\alpha)^{15}\text{N}$ reaction. We performed a further check of the reaction identification by verifying that the reaction products were (not) detected in the same reaction plane, indicating a two (three)-body reaction.

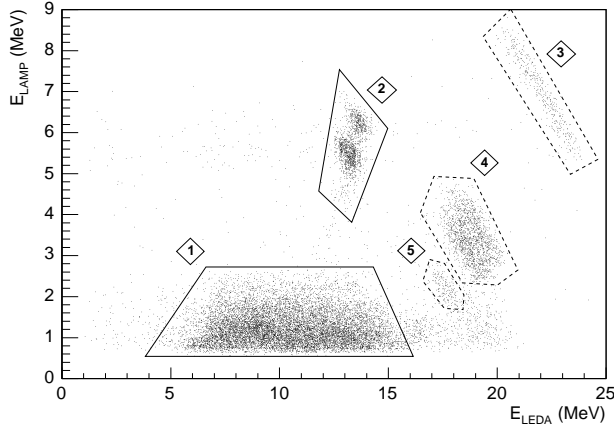


Fig. 3. $E_{LAMP} \times E_{LEDA}$ coincidence spectrum showing several regions corresponding to the $\text{d}(^{18}\text{F},\text{p})^{19}\text{F}$ (solid lines regions) and $\text{d}(^{18}\text{F},\alpha)^{16}\text{O}$ (dashed lines regions) reactions. Label 1 indicates the $\text{d}(^{18}\text{F},\text{p}\alpha)^{15}\text{N}$ reaction while label 2 indicates the $\text{d}(^{18}\text{F},\text{p})^{19}\text{F}$ reaction for ^{19}F excited states below the α -threshold. Label 3, 4 and 5 correspond to different ^{16}O excited states for the $\text{d}(^{18}\text{F},\alpha)^{16}\text{O}$ reaction.

Kinematical bands (energy versus strip number in LAMP) corresponding to the events in Fig 3 are plotted in Fig 4 (right). For comparison, kinematical bands from single events are also plotted in Fig 4 (left). The same patterns as for coincidence events are observed but, in addition, since there is no coincidence condition, some kinematical bands are completed (region 2) or new (between 2 and 4 MeV).

Protons from the $\text{d}(^{18}\text{F},\text{p}\alpha)^{15}\text{N}$ reaction are detected in LAMP in coincidence with α -particle or ^{15}N in LEDA. Both type of coincidences can be separated using the time-of-flight information in LEDA, but since the $\text{p}-\alpha$ coincidences represented only 7% of the total coincidence events, only the $\text{p}-^{15}\text{N}$ coincidences were analysed. After selection of the $\text{p}-^{15}\text{N}$ coincidences, the excitation energy of the decaying ^{19}F levels can be kinematically reconstructed from the energies and angles of the detected protons and the known beam energy. From the ^{19}F excitation energy spectra, and after identifying the populated levels, the differential cross section in the center-of-mass system was calculated following the formula:

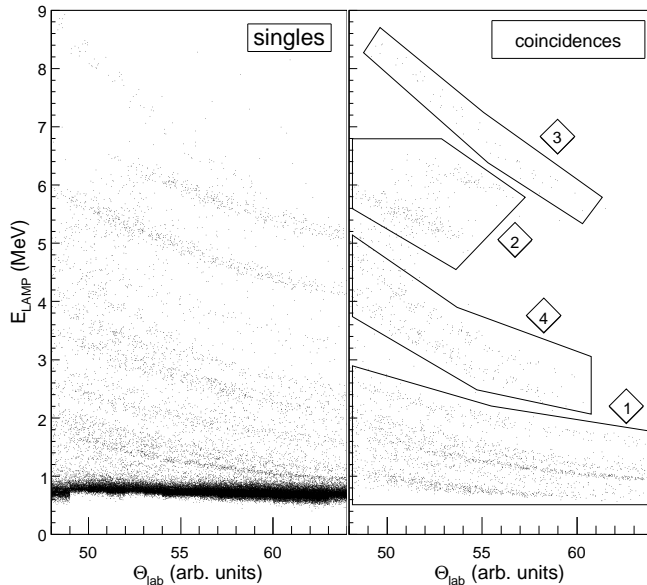


Fig. 4. Kinematical bands in LAMP for single and coincidence events. Angles are given in arbitrary units. Labels have the same meaning as in Fig 3. The different slopes for the kinematical bands (region 4 and 1) is the signature of different reactions [$d(^{18}\text{F},\alpha)^{16}\text{O}$ and $d(^{18}\text{F},p)^{19}\text{F}$, respectively].

$$\left(\frac{d\sigma}{d\Omega}\right)(\theta) = \frac{N_p}{N_{^{18}\text{F}} N_d \Delta\Omega}$$

where N_p is the number of detected protons in a given LAMP strip corresponding to the angle θ , $N_{^{18}\text{F}}$ and N_d are the number of incident ^{18}F ions and the deuteron content of the target per unit area, respectively, and $\Delta\Omega$ is the geometrical solid angle. In the case of coincidences, $\Delta\Omega$ is multiplied by the $p\text{-}^{15}\text{N}$ coincidence efficiency which is determined by Monte-Carlo simulations considering an isotropic angular distribution in the $\alpha\text{-}^{15}\text{N}$ center-of-mass system for the α -decay of the ^{19}F . However for the two $3/2^+$ levels, the α -particle is emitted with an $\ell = 1$ angular momentum. Monte-Carlo simulations using α -particle angular distribution corresponding to different sub-magnetic population, gave an uncertainty related to the normalisation of about 15%.

3. Spectra and peak deconvolution

3.1. ^{19}F Spectra

The reconstructed ^{19}F excitation energy spectra are shown in Figure 5 for coincidence (bottom) and single (top) events after applying the alpha calibration and before the internal calibration (see the end of the subsection for more details). Owing to the high coincidence efficiency ($\epsilon = 70\%$), the coincidence and singles counting statistics were comparable. Both spectra correspond to all the events collected in the 6 sectors of the

LAMP detector without any correction for the beam position on target. Because LAMP is very close to the target, this reconstruction is very sensitive to the beam position on the target, which is known within ± 2 mm. Hence the angular position of the strips on a same ring varies, inducing a different reconstructed excitation energy for the same detected proton energy. This, in turn, leads to a deterioration of the resolution when the contribution of the 6 LAMP sectors are directly summed without correction. To compensate this effect, the 6.5 MeV peak obtained in coincidence for each LAMP sector is fitted and each spectrum is shifted relative to the mean position of the 6 sectors.

For the coincidence events, the vertical lines in Figure 5 (bottom) present the position of the ^{19}F levels [26] populated with low transferred angular momentum ($\ell \leq 2$). Even if the energy resolution (FWHM ≈ 100 keV) is not sufficient to separate the 20 ^{19}F levels that are represented, the two $3/2^+$ levels of interest in ^{19}F at $E_x = 6.497$ and 6.528 MeV (the analogs of the $3/2^+$ levels in ^{19}Ne) are well isolated from the other groups of levels. Unlike for coincidence events, single events (Figure 5 top) are directly selected from a time-of-flight versus energy spectrum in LAMP, which does not allow to separate proton events from α -particle events coming from the $d(^{18}\text{F},\alpha)^{16}\text{O}$ reaction. For ^{19}F excitation energies higher than about 5 MeV, one can observe the same structure for the single and coincidence spectrum. However, it should be noted that the 7.2-7.3 MeV peak is less populated than in the coincidence spectrum because a higher energy threshold for the selection of single events is used to reduce electronic noise. For lower excitation energy (below the α -threshold), ^{19}F levels are observed down to the ground state and the vertical lines represent all the existing ^{19}F levels.

We performed an internal excitation energy calibration using the peaks corresponding to the well isolated ^{19}F levels at $E_x = 2.780$ MeV, 5.106 MeV as well as the doublet $E_x = 7.262 + 7.363$ MeV. In case of the unresolved peak at 7.3 MeV, its doublet nature was checked by performing a fit with two components where the position of each component was left as a free parameter. The experimental energy difference obtained ($\Delta E_x = 107$ keV) is in very good agreement with the energy difference from the literature ($\Delta E_x = 101$ keV) and the hypothetical presence of a third state in this energy region [17] was not needed to describe the data.

3.2. Peak deconvolution

The ^{19}F excitation energy spectrum obtained after the internal calibration is shown in Figure 6 as well as a fit to the data between $E_x = 6150$ and 6950 keV. The fit includes the contribution of two levels for the 6.5 MeV peak ($E_x = 6497 + 6527$ keV), three levels for the 6.25 MeV peak ($E_x = 6255 + 6282 + 6330$ keV) and three levels for the 6.9 MeV peak ($E_x = 6787 + 6838 + 6891$ keV). The free parameters of the fit are the amplitude of each gaussian and a width common to all the levels. The level energies are fixed. The excess of counts below the 6.5 MeV peak is interpreted as the broad $1/2^-$ level $E_x = 6536$ keV [27] ($\Gamma = 245$ keV) for which only the intensity is left as a free parameter.

For this broad ^{19}F $1/2^-$ level, we used the values of the energy and width derived recently [27] from a reanalysis of previous data [28]. Compared to previous adopted values, the width is similar (245 keV instead of 280 keV) but the energy is about 100 keV higher ($E_x = 6536$ keV instead of $E_x = 6429$ keV). It should be noted that the fit obtained with the new parameters is better ($\chi^2/\text{ndf} = 1.19$) than with the previous parameters

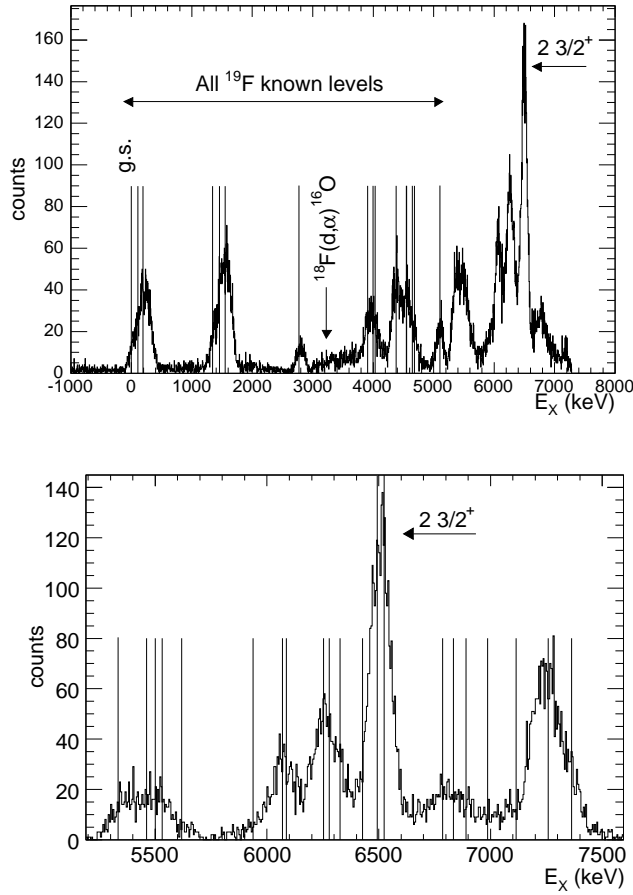


Fig. 5. *Top*: Reconstructed ^{19}F spectrum for single events after the alpha calibration. Levels down to the ground state are populated. Contribution from the $d(^{18}\text{F},\alpha)^{16}\text{O}$ reaction is shown (see text for details) *Bottom*: Same for coincidence events, but covering only excitation energies above the α -particle emission threshold. The doublet of $3/2^+$ astrophysical levels around 6.5 MeV is well isolated from the other levels. Vertical lines show ^{19}F levels (see text).

($\chi^2/\text{ndf} = 1.54$, see Figure 1 in [29]). Furthermore, a fit with the same conditions but with the energy of the broad $1/2^-$ level as free parameter naturally gives an energy of $E_x = 6529 \pm 13$ keV, compatible with the new value from [27].

The solid line on Figure 6 shows the best fit and the dashed lines represent the contribution of each level separately. For the 6.5 MeV peak composed of the two $3/2^+$ levels, the high-energy level is favored with a relative contribution of 5%–95% for the $E_x = 6497$ and 6527 keV level respectively. A recent experiment using the same reaction but a higher bombarding energy found an opposite proportion for the two $3/2^+$ levels [17]. In both cases, an internal energy calibration of the ^{19}F excitation energy was used. The differences are that our energy calibration is an interpolation based on experimental peaks surrounding the $3/2^+$ levels of astrophysical interest whereas in Ref. [17] the calibration

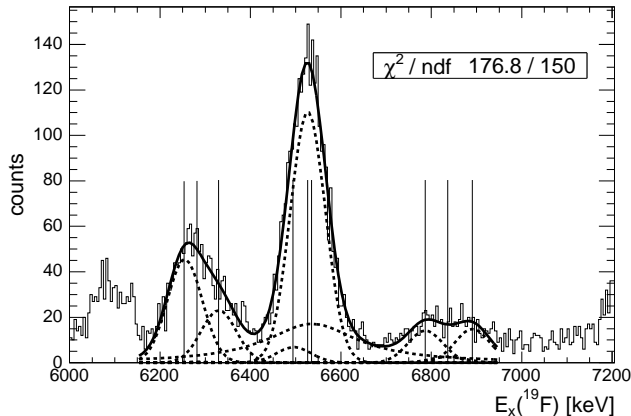


Fig. 6. Reconstructed ^{19}F coincidence spectrum after applying the internal energy calibration. The solid line represents the best fit of the spectrum and the vertical lines indicate the involved levels. Each level contribution is shown in dashed lines. See text for details.

is an extrapolation done for several laboratory angles, from peaks at lower energies than the levels of astrophysical interest.

However, since the two levels are not experimentally resolved, different relative contributions can give similar χ^2 and hence the nominal relative contribution derived above should be taken with care. Hence we performed a statistical study aiming at the determination of the upper limit of the $E_x = 6497$ keV level contribution. A careful study of the systematic errors (target thickness and detector dead layer, beam energy, energy loss in the target and in the detector dead layer, beam centering and detector position) associated to the reconstruction of the excitation energy, showed that the most important uncertainty is related to the precise position of the LAMP detector. Hence three uncertainties were taken into account: the error associated to the internal energy calibration (≈ 3 keV for $E_x \approx 6.5$ MeV), the error associated to the precise position of LAMP after the internal energy calibration (≈ 5 keV for ± 1 mm) and the deconvolution procedure of the 6.5 MeV peak. The $1-\sigma$ upper limit for the contribution of the $E_x = 6497$ keV level for each effect taken separately is 41%, 34% and 44% respectively. When summed quadratically, we obtain a contribution for the $E_x = 6497$ keV level of $5^{+65}_{-5}\%$. It should be noted that there is a $7/2$ level of unknown parity at $E_x = 6554$ keV lying just above the $3/2^+$ doublet. We estimated its contribution to be less than 5%.

From the previous analysis, one cannot exclude that the two $3/2^+$ levels are populated in the same proportion. However one expects that these two levels have different structure properties as it is suggested by an electron inelastic scattering measurement on ^{19}F [30]. Such an experiment gives access to the transversal and longitudinal form factors $[F^2(q)]$ as a function of the transferred momentum q^2 . For such an inelastic scattering, the form factor depends on the initial and final nuclear states and hence of the nuclear structure of the observed levels. The longitudinal form factor of the two $3/2^+$ levels are different by more than one order of magnitude, indicating a very different nuclear structure. It is then not surprising that one of the two levels would be preferentially populated through the $d(^{18}\text{F},p)^{19}\text{F}$ transfer reaction, since transfer reactions are very sensitive to the nuclear

structure.

4. DWBA and compound nucleus components

4.1. DWBA parameters

DWBA calculations were performed with the FRESKO code [31] in Finite-Range. For testing the dependency of the results versus the DWBA parameters, two sets of optical parameters were used: A+A' and B+B' (see Table 1). The optical potentials are written as usual:

$$V_{opt} = V_C - V_0 f(r, r_0, a_0) - i \left[W f(r, r_W, a_W) - 4W_D \frac{d}{dr} f(r, r_D, a_D) \right] + \frac{V_{s.o.}}{r} \left(\frac{\hbar}{m_\pi c} \right) \boldsymbol{\sigma} \cdot \mathbf{L} \frac{d}{dr} f(r, r_{s.o.}, a_{s.o.})$$

where $f(r, r_i, a_i)$ is a potential well of Wood-Saxon shape with r_i and a_i being the radius and the diffuseness of the interaction potentials. V_C , V_0 , W , W_D and $V_{s.o.}$ are the Coulomb, the volume, the volume absorption, the surface absorption and the spin-orbit well depths, respectively. Usually the optical parameters are determined by fitting elastic scattering data of the entrance and exit channels. Such data do not exist for the $d+^{18}\text{F}$ channel, so here the parameters correspond to other nuclear systems of similar masses and similar energies. The first set of parameters A+A' comes from a compilation [32], whereas the second set of parameters B+B' comes from a similar neutron transfer reaction $^{19}\text{F}(d,p)^{20}\text{F}$ which was studied at the same center-of-mass energy [33]. In that study, 11 angular distributions of ^{20}F excited states are well described by the optical potential B+B'. For the Finite-Range calculation, the potential describing the deuteron is of Reid Soft Core type [34]. The depth of the volume potential well for the transferred neutron is automatically adjusted to reproduce its separation energy in ^{19}F .

Table 1

Optical potential parameters used for the DWBA analysis. Potentials A+A' are from [32] and B+B' are from [33]. Notations are explained in the text.

Optical potentials	r_C (fm)	V_0 (MeV)	r_0 (fm)	a_0 (fm)	W (MeV)	r_W (fm)	a_W (fm)	W_D (MeV)	r_D (fm)	a_D (fm)	$V_{s.o.}$ (MeV)	$r_{s.o.}$ (fm)	$a_{s.o.}$ (fm)
$^{18}\text{F} + d$ entrance channel													
A	1.3	80.1	1.1	0.972	—	—	—	14.8	1.6	0.652	—	—	—
B	1.3	60.0	1.5	0.6	20	1.5	0.6	—	—	—	—	—	—
$^{19}\text{F} + p$ exit channel													
A'	1.3	47.45	1.185	0.721	—	—	—	7.5	0.942	0.568	5.1	1.042	0.488
B'	1.3	50.0	1.3	0.5	—	—	—	8	1.3	0.5	—	—	—

It should be noted that even if the energy available in the center-of-mass system (1.4 MeV) of the $d(^{18}\text{F}, p\alpha)^{15}\text{N}$ reaction is lower than the Coulomb barrier ($E_C =$

2.6 MeV), the emitted protons from the two $3/2^+$ levels of astrophysical interest are slightly above the Coulomb barrier of the exit channel ($E_p = 3.1$ MeV and $E_C = 2.7$ MeV). Hence the term of “sub-Coulomb transfer” does not seem to be justified for the conditions of this reaction. We have checked this by computing a DWBA calculation in which the nuclear potentials were switched off, only leaving a Coulomb potential. This calculation was unable to reproduce the shape of the angular distribution for the two $3/2^+$ levels.

4.2. Compound nucleus component

Due to the restricted angular range ($\theta_{c.m.} < 50^\circ$), we used the $9/2^+$ $E_x = 2780$ keV ^{19}F level observed in our data to estimate the compound nucleus component. Its spin and parity make it difficult to be populated by a transfer reaction due to the high transferred angular momentum $\ell = 4$ which corresponds to a 9.2 MeV centrifugal barrier, to be added to the Coulomb barrier. The DWBA calculation for this level with a maximum spectroscopic factor of 1 (see Figure 7) fails to describe the data. Two-step processes such as the excitation of the 3^+ state at 937 keV in ^{18}F followed by the transfer of a neutron into an $\ell = 2$ orbital were also computed with the coupled channels code CCZR [35]. The contribution of these two-step processes was at most a few $\mu\text{b}/\text{sr}$ and can not explain the angular distribution of the $9/2^+$ level. The Hauser-Feshbach contribution was calculated with the HSF3 [36] code taking into account the open channels from the compound nucleus ^{20}Ne decay at our bombarding energy and normalized to the $E_x = 2780$ keV data. Applying this normalization to the $5/2^+$ $E_x = 5106$ keV ^{19}F level describes successfully the data which does not seem to be described by a dominant direct reaction mechanism (see Figure 7).

5. Discussion

The angular distributions of single data for the $E_x(^{19}\text{F}) = 2780$ and 5106 keV levels and of coincidence data for the doublet $E_x(^{19}\text{F}) = 6497$ and 6527 keV and the two $E_x(^{19}\text{F}) = 7262$ and 7364 keV levels are shown in Figure 7. While the angular distributions for the two levels at $E_x = 2780$ and 5106 keV are quite flat, supporting a compound nucleus type reaction mechanism, the angular distribution of the $3/2^+$ doublet shows a strong variation of about one order of magnitude in a small center-of-mass angular range, which is typical of a direct reaction mechanism. The spectroscopic factors obtained from our analysis are displayed in Table 2.

5.1. Levels at $E_x = 6.497$ and 6.527 MeV in ^{19}F

The two $3/2^+$ levels can be populated by both $\ell = 0$ and $\ell = 2$ transfers, however the fit of the DWBA calculations to the data indicates that only the $\ell = 0$ component is contributing (see Figure 7) at such low center of mass energy. At much higher incident energy, a $\ell = 2$ component was requested to reproduce transfer data [17]. Taking into account the compound nucleus contribution as explained above, we obtain for $\ell = 0$ a spectroscopic factor of $S(6.497 + 6.527) = 0.17$ (to be compared with $S = 0.12$ from a recent experiment [17]). This value supersedes our previous value of $S(6.497 + 6.527) =$

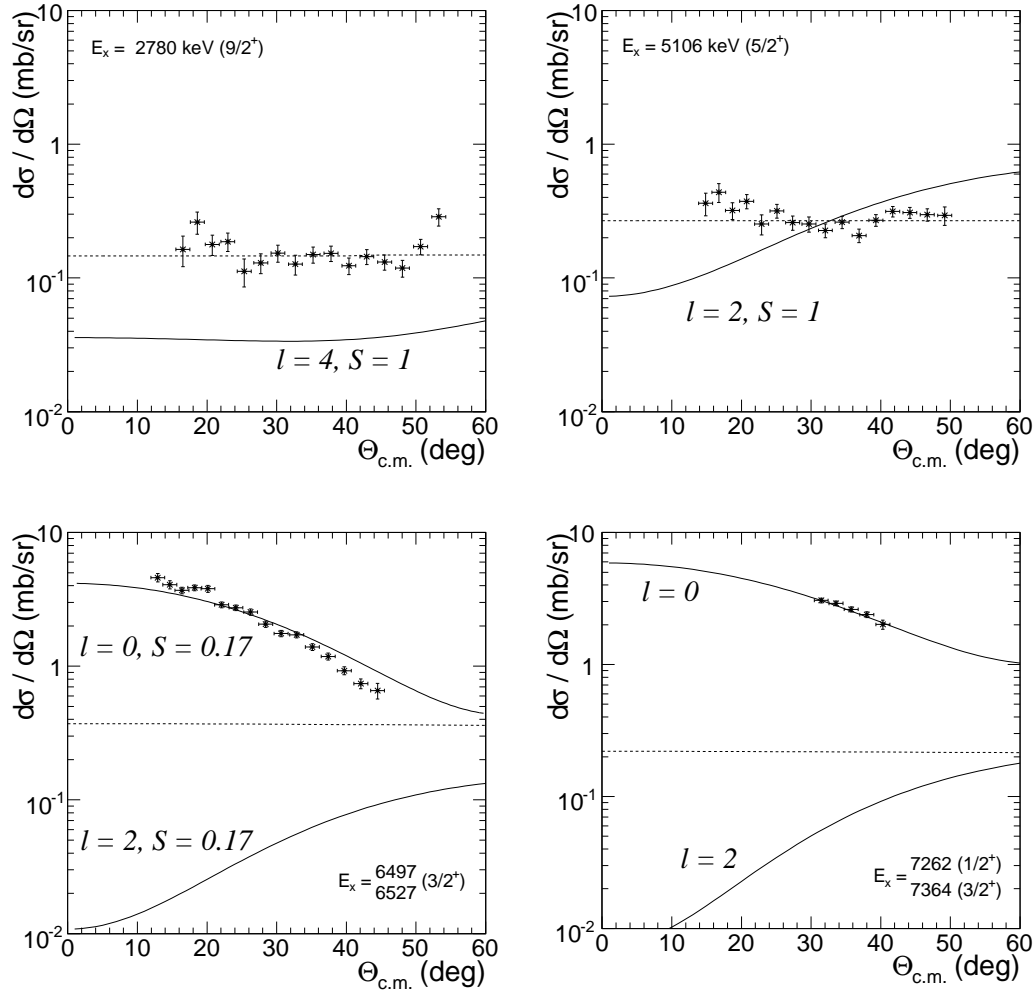


Fig. 7. Angular distributions for the ^{19}F levels at 2.780, 5.106 MeV, the doublet at 6.497 and 6.537 MeV, and the levels at 7.262 and 7.364 MeV, populated by the $d(^{18}\text{F},p)^{19}\text{F}$ transfer reaction. Dashed lines represent the compound nucleus component and solid line are the results of the direct contribution calculated using a Finite-Range DWBA analysis and the B+B' optical potentials.

0.21 [15]: the difference comes from the new Finite-Range DWBA calculations and the inclusion of the Hauser-Feshbach contribution. The fact that the two sets of optical parameters A+A' and B+B' give very similar angular distributions and spectroscopic factors makes us to feel confident about the present results. The analysis of the single data events for this $3/2^+$ doublet allowed us to derive the corresponding angular distribution and to compare it with the coincidence one. They agree well, both in the shape and in the normalisation, hence giving strong confidence in the coincidence solid angle determined by Monte-Carlo simulations.

The uncertainties associated to the spectroscopic factors have been evaluated to be

Table 2
Spectroscopic factors for the ^{19}F levels analyzed in DWBA.

$E_x(^{19}\text{F})$ [MeV]	J^π	ℓ_n	C^2S
6.497	3/2 ⁺	0	0.17
6.527			
6.536	1/2 ⁻	1	< 0.33
7.262	3/2 ⁺	0	0.15
7.363	1/2 ⁺	0	0.22

of 25%. The major source of uncertainty comes from the DWBA method (20%) and is related to the choice of the optical parameters in the entrance channel which cannot be constrained by experimental data. Another source of uncertainty (15%), which has already been discussed, arises from the angular distribution of the emitted α -particle in the ^{19}F center-of-mass frame. The uncertainty on the normalization contributes to 7% (Section 3).

5.2. Level at $E_x = 6.536$ MeV in ^{19}F

Due to its large total width $\Gamma = 245$ keV [27], this 1/2⁻ level can play an important role in the $^{18}\text{F}(p,\alpha)^{15}\text{O}$ reaction since it covers the whole Gamow peak at novae temperatures. But its large width also makes it difficult to be observed. However, making the hypothesis that all the excess of counts below the 6.5 MeV peak comes from the 1/2⁻ level, an upper limit to its contribution could be derived. This hypothesis does not seem unrealistic because no counts are observed in the coincidence spectrum in the $E_x = 5.8$ MeV region (see Figure 5 bottom), where no ^{19}F levels exist. Hence this seems to indicate that the excess of counts below the 6.5 MeV peak has a physical origin.

The number of counts corresponding to the population of the 1/2⁻ level is obtained from the global fit presented in Figure 6 where this level is described by a lorentzian shape whose amplitude is a free parameter. Then, assuming a $\ell = 1$ transfer for populating this level, one obtains an upper limit for the spectroscopic factor of $S(6.536) < 0.33$. The difference with respect to our previous value ($S(6.536) < 0.15$ [15]) comes from the new position and width of this level [27] as well as from the DWBA calculation, now made in Finite-Range.

5.3. Levels at $E_x = 7.262$ and 7.364 MeV in ^{19}F

The experimentally unresolved ^{19}F levels at 7.262 and 7.364 MeV have a 3/2⁺ and 1/2⁺ spin and parity, respectively, and both can be populated by a $\ell = 0$ or $\ell = 2$ neutron transfer. However the DWBA calculations fitted to the data showed that only the $\ell = 0$ is contributing (see Figure 7). These two levels have the highest excitation energy which can be achieved with the beam energy used here, and correspond to the less energetic protons detected ($E_p < 1$ MeV). Part of the kinematical band of these two levels, which are not experimentally resolved, is cut by the electronic threshold. Hence only the five outer strips of LAMP were considered in the analysis. The extracted angular distribution does not allow to deduce the relative contribution of the two levels

since the differential cross section has the same shape due to the same $\ell = 0$ transfer but a different normalisation (a factor of 2) due to the spin factor. However a two-peak fitting analysis of the 7.3 MeV excitation energy peak indicates a relative contribution of 57%–43% for the 7.262 and 7.364 MeV levels, allowing to obtain a set of spectroscopic factors $S(7.262) = 0.15$ and $S(7.364) = 0.22$. The compound nucleus component which has been taken into account has a negligible cross section (≈ 0.1 mb/sr).

5.4. Analog level of the $E_x(^{19}\text{Ne}) = 7.076$ MeV

Up to now, the analog level in ^{19}F of the $^{18}\text{F}(p,\alpha)^{15}\text{O}$ resonance at $E_r = 665$ keV [$E_x(^{19}\text{Ne}) = 7.076$ MeV, $J^\pi = 3/2^+$] is still not identified. A gamma-ray measurement [37] via the $^{15}\text{N}(\alpha,\gamma)^{19}\text{F}$ reaction found a level at 7.101 MeV in ^{19}F with a width $\Gamma_\alpha = 28$ keV. The spin and parity was deduced to be $3/2^+$ by observing gamma-ray transitions to a $3/2^-$ level. Assuming equality of reduced α -widths between analog states, Butt et al. [37] find $\Gamma_\alpha \approx 30$ keV for the ^{19}Ne level at $E_x = 7.076$ MeV, which is in good agreement with the value of $\Gamma_\alpha = 24$ keV from [9].

However, the assignation of a $3/2^+$ spin and parity to the $E_x(^{19}\text{F}) = 7.101$ MeV level has been questioned by Fortune and Sherr [38] who pointed out that this level could be a doublet of spins $1/2-5/2$ or $1/2-7/2$. Furthermore, these authors predict the position of the analog level at higher energy around $E_x = 7.4 \pm 0.1$ MeV.

Assuming here that the 7.101 MeV level in ^{19}F is the analog of the $E_x(^{19}\text{Ne}) = 7.076$ MeV and assuming equality between dimensionless reduced widths [$\Theta_n^2(^{19}\text{F}) = \Theta_n^2(^{19}\text{Ne})$], we obtain $\Theta_n^2(^{19}\text{F}) = 0.14$. This value is comparable to the one from the two $3/2^+$ levels of astrophysical interest ($\Theta_n^2 = 0.1$) and should hence appear in our spectra as a peak of similar intensity as the 6.5 MeV peak, but our data (Figure 5, bottom) do not show any evidence of a peak around 7.1 MeV. Furthermore it has been shown recently that the spin of this resonance was unlikely to be $3/2^+$ [27].

The 7.3 MeV group in ^{19}F is composed of two states at 7.262 MeV ($3/2^+$) and 7.368 MeV ($1/2^+$) whose spectroscopic factors are determined here to be $S = 0.15$ and 0.22 , respectively (see Table 2). The spectroscopic factor value for the $3/2^+$ state is very close to the one of the level at 7.076 MeV in ^{19}Ne , and seems then to indicate that the $E_x(^{19}\text{F}) = 7.262$ MeV is a good candidate for the analog level of the 7.076 MeV in ^{19}Ne . However, it should be noted that the total width of the 7.262 MeV level in ^{19}F calculated from the $E_x(^{19}\text{Ne}) = 7.076$ MeV is $\Gamma = \Gamma_\alpha \approx 28$ keV which seems incompatible with the measured value $\Gamma < 6$ keV [26].

5.5. Proton widths in ^{19}Ne

The obtained neutron spectroscopic factors are for ^{19}F levels whereas the proton widths of astrophysical interest correspond to their analog levels in ^{19}Ne . Following Utku et al. [14], we assume that the two $3/2^+$ levels $E_x = 6497$ and 6527 keV and the $1/2^-$ level $E_x = 6536$ keV populated in ^{19}F are the analog states of the $3/2^+$ levels $E_x(^{19}\text{Ne}) = 6419$ and 6449 keV, and of the $E_x(^{19}\text{Ne}) = 6437$ keV, respectively, even if the spins and parity of ^{19}Ne states has not been determined experimentally. Unlike other analog levels in $^{19}\text{F}/^{19}\text{Ne}$ where the assignation comes from the fact that the levels are populated with comparable statistics by mirror reactions, the case of the two $3/2^+$ and $1/2^-$ levels only

relies on the similarity of their energy position and of their total width, respectively. The two $3/2^+$ levels are both separated by 30 keV in ^{19}F and ^{19}Ne at similar excitation energies, whereas for the $1/2^-$ level $\Gamma_\alpha(^{19}\text{Ne}) = 220 \text{ keV} \approx \Gamma_\alpha(^{19}\text{F}) = 245 \text{ keV}$.

It is of common use in nuclear astrophysics to assume equality of spectroscopic factors between analog states. Hence for the $3/2^+$ states in ^{19}Ne , we obtain a proton spectroscopic factor $S = 0.17$ and for the $1/2^-$ state, we obtain an upper limit $S < 0.33$. However, the uncertainty associated to this practice is estimated to be a factor of two from the comparison of the values of neutron and proton spectroscopic factors for all the analog states of the sd shell nuclei (Figure 8).

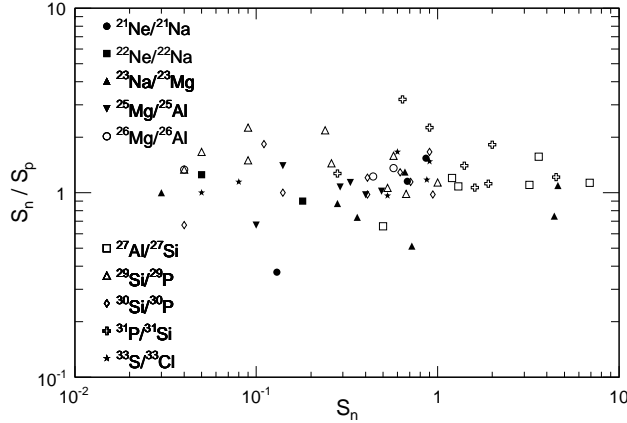


Fig. 8. Comparison of neutron and proton spectroscopic factors for analog levels of the sd shell nuclei. Data comes from [19].

The proton widths are calculated using the following relations:

$$\Gamma_p = C^2 S \Gamma_{s.p.} \quad \text{with} \quad \Gamma_{s.p.} = \frac{\hbar^2 s}{\mu} |\mathcal{R}_{s.p.}(s)|^2 P_l,$$

where $\Gamma_{s.p.}$ is the single-particle width, s is the interaction radius ($s = 4.5 \text{ fm}$) and $\mathcal{R}_{s.p.}$ is the proton radial wave function in the $p+^{18}\text{F}$ system calculated with classical parameters for the Wood-Saxons nuclear potential: $(r, a) = (1.25, 0.65) \text{ fm}$, where r and a are the radius and diffuseness of the potential. As compared to direct determination of the proton width, a statistical study of sd shell nuclei showed an agreement between direct and indirect method of about 30% [39]. Using the above prescription we obtain for the $3/2^+$ doublet in ^{19}Ne , $\Gamma_p(6.419) = 3.4 \times 10^{-37} \text{ keV}$ and $\Gamma_p(6.449) = 1.9 \times 10^{-37} \text{ keV}$ assuming that the total strength of the doublet is put on each level respectively. As far as the levels above $E_x = 7 \text{ MeV}$ are concerned and if we assume that the levels $E_x(^{19}\text{F}) = 7.262 \text{ MeV}$ and $E_x(^{19}\text{Ne}) = 7.238 \text{ MeV}$ are analogs [14] we obtain $\Gamma_p(7.238) = 10.3 \text{ keV}$ which is larger than the adopted upper limit ($\Gamma_p < 4 \text{ keV}$ [14]). For the analog state of the $E_x(^{19}\text{F}) = 7.364 \text{ MeV}$ $1/2^+$ level, no $1/2^+$ levels in ^{19}Ne have been observed so far at an excitation energy around 7.3 MeV.

6. CONCLUSIONS: REMAINING UNCERTAINTIES

Our analysis showed that the two expected low-lying 8 keV and 38 keV proton resonances ($E_x = 6419$ and 6449 keV in ^{19}Ne) must be considered for the calculation of the $^{18}\text{F}(\text{p},\alpha)^{15}\text{O}$ reaction. Here we focus on the remaining uncertainties before firm reaction rates can be computed for the $^{18}\text{F}(\text{p},\alpha)^{15}\text{O}$ and $^{18}\text{F}(\text{p},\gamma)^{19}\text{Ne}$ reactions.

Due to the small energy difference (30 keV) between the two $3/2^+$ levels in ^{19}F ($E_x = 6497$ and 6527 keV) and the two resonances in ^{19}Ne ($E_r = 8$ and 38 keV), the assignment of analog pairs is not straightforward and one cannot discard the possibility of an inversion. Hence the identification of the main contributing ^{19}F level is not so crucial for the determination of the associated proton widths in ^{19}Ne . So two cases will have to be considered, the whole strength at the $E_r = 8$ keV resonance or at the $E_r = 38$ keV resonance.

The second uncertainty arise from interference effects between the two $E_r = 8$ and 38 keV resonances and the $3/2^+$ resonance at $E_r = 665$ keV (corresponding to the ^{19}Ne level $E_x = 7.076$ MeV). The sign of these interferences is totally unknown and for the destructive case, the S-factor would become extremely small between 100 and 300 keV, which corresponds to Gamow peak energies for temperatures achieved in novae ($50 < T_6 < 350$). As usual, the notation $T_x = y$ corresponds to the temperature $y \times 10^x$ K.

Another uncertainty on the reaction rates comes from the poor knowledge of the ^{19}Ne alpha widths, Γ_α , for the $E_r = 8$ and 38 keV resonances. Since there are no measurements of these Γ_α in ^{19}Ne , they are usually deduced from the analog states in ^{19}F . However differences as large as a factor 10 have been observed for alpha widths of analog levels for the $^{19}\text{F} / ^{19}\text{Ne}$ mirror nuclei [40]. Calculations of constructive and destructive interferences for different values of alpha widths showed a strong impact on the $^{18}\text{F}(\text{p},\alpha)^{15}\text{O}$ reaction rate [41].

Finally the energy of the two $E_r = 8$ and 38 keV resonances in ^{19}Ne is not known better than 6 keV [14]. This effect is far less important than the one of the unknown alpha widths because the position of the resonances are below the energies corresponding to the Gamow peak for temperatures relevant to ^{18}F production in novae.

In conclusion we reported here on our latest results concerning the one-nucleon transfer reaction $\text{d}(^{18}\text{F},\text{p}\alpha)^{15}\text{N}$ used to study ^{19}F analog states of the astrophysically important states in ^{19}Ne . A DWBA analysis of the data showed that the two $3/2^+$ low-energy resonances in ^{19}Ne , $E_r = 8$ and 38 keV have a relatively large spectroscopic factor ($S = 0.17$) and hence cannot be neglected in calculating the $^{18}\text{F}(\text{p},\alpha)^{15}\text{O}$ and $^{18}\text{F}(\text{p},\gamma)^{19}\text{Ne}$ reaction rates. We made a careful analysis of the impact on the reaction rates of remaining uncertainties. This includes interferences between the low-lying states and the $3/2^+$ $E_r = 665$ keV resonance, the unknown α -widths in ^{19}Ne and the possibility of inversion for the analog levels between ^{19}F and ^{19}Ne . A new challenging experiment to investigate the $^{18}\text{F}(\text{p},\alpha)^{15}\text{O}$ reaction at energies below 0.6 MeV in the center-of-mass will be soon performed at the Louvain-la-Neuve CYCLONE facility.

Acknowledgments This work has been supported by the European Community-Access to Research Infrastructure action of the Improving Human Potential Program, contract

N HPRI-CT-1999-00110, and the Belgian Inter-University Attraction Poles P05/07. One of us (P.L.) is a Research Director of the National Fund for Scientific Research, Brussels. We wish to thank Jean-Pierre Thibaud for very fruitful discussions concerning the data analysis and his careful reading of the manuscript. We also thank Jordi José and Margarita Hernanz for very interesting discussions concerning the astrophysical implications of the present work.

References

- [1] J. Gómez-Gomar, M. Hernanz, J. José, et al. *MNRAS* 296 (1998) 913.
- [2] M. Hernanz, J. José, A. Coc, et al. *Astrophys. J.* 526 (1999) L97.
- [3] A. Coc, M. Hernanz, J. José, et al. *Astron. Astrophys.* 357 (2000) 561.
- [4] C. Fox, C. Iliadis, A. E. Champagne, et al. *Phys. Rev. Lett.* 93 (2004) 081102.
- [5] C. Fox, C. Iliadis, A. E. Champagne, et al. *Phys. Rev.* C71 (2005) 055801.
- [6] A. Chafa, V. Tatischeff, P. Aguer, et al. *Phys. Rev. Lett.* 95 (2005) 031101.
- [7] D. W. Bardayan, J. C. Blackmon, W. Bradfield-Smith, et al. *Phys. Rev.* C62 (2000) 42802.
- [8] J.-S. Graulich, S. Cherubini, R. Coszach, et al. *Phys. Rev.* C63 (2001) 11302.
- [9] D. W. Bardayan, J. C. Blackmon, W. Bradfield-Smith, et al. *Phys. Rev.* C63 (2001) 65802.
- [10] R. Coszach, M. Cogneau, C. R. Bain, et al. *Phys. Lett.* B353 (1995) 184.
- [11] K. E. Rehm, M. Paul, A. D. Roberts, et al. *Phys. Rev.* C52 (1995) 460.
- [12] J.-S. Graulich, F. Binon, W. Bradfield-Smith, et al. *Nucl. Phys.* A626 (1997) 751.
- [13] D. W. Bardayan, J. C. Batchelder, J. C. Blackmon, et al. *Phys. Rev. Lett.* 89 (2002) 262501.
- [14] S. Utku, J. G. Ross, N. P. T. Bateman, et al. *Phys. Rev.* C57 (1998) 2731.
- [15] N. de Séréville, A. Coc, C. Angulo, et al. *Phys. Rev.* C67 (2003) 052801 (R).
- [16] D. W. Visser, J. A. Caggiano, R. Lewis, et al. *Phys. Rev.* C69 (2004) 048801.
- [17] R. L. Kozub, D. W. Bardayan, J. C. Batchelder, et al. *Phys. Rev.* C71 (2005) 032801 (R).
- [18] B. A. Brown, A. Etchegoyen, and W. D. M. Rae. The computer code OXBASH, MSU-NSCL Report No. 524 (1988).
- [19] A. M. Lane. *Rev. Mod. Phys.* 32 (1960) 519.
- [20] M. H. Macfarlane and J. B. French. *Rev. Mod. Phys.* 32 (1960) 567.
- [21] M. Cogneau, P. Decrock, M. Gaelens, et al. *Nucl. Inst. and Meth.* A420 (1999) 489.
- [22] H. Bernas, J. Chaumont, E. Cottureau, et al. *Nucl. Inst. and Meth.* B62 (1992) 416.
- [23] R. Amikiras, D. N. Jamieson, and S. P. Dooley. *Nucl. Inst. and Meth.* B77 (1993) 110.
- [24] D. C. Kocher and T. B. Clegg. *Nucl. Phys.* A132 (1969) 455.
- [25] T. Davinson, W. Bradfield-Smith, S. Cherubini, et al. *Nucl. Inst. and Meth.* A454 (2000) 350.
- [26] D. R. Tilley, H. R. Weller, C. M. Cheves, et al. *Nucl. Phys.* A595 (1995) 1.
- [27] D. W. Bardayan, R. L. Kozub, and M. S. Smith. *Phys. Rev.* C71 (2005) 018801.
- [28] H. Smotrich, K. W. Jones, L. C. McDermott, et al. *Phys. Rev.* 122 (1961) 232.
- [29] N. de Séréville, E. Berthoumieux, and A. Coc. *Nucl. Phys.* A478 (2005) 745c.

- [30] B. A. Brown, B. H. Wildenthal, C. F. Williamson, et al. Phys. Rev. C32 (1985) 1127.
- [31] I. J. Thompson. *Computer Physics Report* 7 (1988) 167.
- [32] C. M. Perey and F. G. Perey. Atomic Data and Nuclear Data Tables 17 (1976) 1.
- [33] M. E. O. de López, J. Rickards, and M. Mazari. Nucl. Phys. 51 (1964) 321.
- [34] R. V. Reid. *Annals of Physics* 50 (1968) 411.
- [35] J. Van de Wiele (1970). IPN Orsay, unpublished.
- [36] M. Mermaz. Sur la séparation des mécanismes de réactions à basse énergie. Étude des réactions $^{27}\text{Al}(d,p)^{28}\text{Al}$, $^{24}\text{Mg}(d,p)^{25}\text{Mg}$ et $^{24}\text{Mg}(d,\alpha)^{22}\text{Na}$ (1967). Rapport CEA - R 3078, unpublished.
- [37] Y. M. Butt, J. W. Hammer, M. Jaeger, et al. Phys. Rev. C58 (1998) 10.
- [38] H. T. Fortune and R. Sherr. Phys. Rev. C61 (2000) 24313.
- [39] S. E. Hale, A. E. Champagne, C. Iliadis, et al. Phys. Rev. C70 (2004) 045802.
- [40] F. de Oliveira, A. Coc, P. Aguer, et al. Phys. Rev. C55 (1997) 3149.
- [41] N. de Séréville. Ph.D. thesis (2003).